JOURNAL OF PHYSICAL ORGANIC CHEMISTRY, VOL. 8, 713–720 (1995)

GROUND- AND EXCITED-STATE PROTOTROPIC TAUTOMERISM IN ANILS OF AROMATIC α-HYDROXYALDEHYDES STUDIED BY ELECTRONIC ABSORPTION, FLUORESCENCE AND ^{1}H AND ^{13}C NMR SPECTROSCOPIES AND SEMI-EMPIRICAL CALCULATIONS

SERGIO H. ALARCÓN AND ALEJANDRO C. OLIVIERI*

Departamento de Química Analítica, Facultad de Ciencias Bioquímicas y Farmacéuticas, Universidad Nacional de Rosario, Suipacha 531, Rosario (2000), Argentina

AND

RAQUEL M. CRAVERO, GUILLERMO LABADIE AND MANUEL GONZÁLEZ-SIERRA*

IQUIOS, Facultad de Ciencias Bioquímicas y Farmacéuticas, Universidad Nacional de Rosario, Suipacha 531, Rosario (2000), Argentina

Proton transfer processes in both the ground and excited states in anils of aromatic α-hydroxyaldehydes (salicylaldehyde, 2-hydroxynaphthalene-1-carbaldehyde and the novel 10-hydroxyphenanthrene-9-carbaldehyde) have been studied by a combination of spectroscopic techniques. Solution ^{1}H and ^{13}C NMR is used to establish the position of the tautomeric equilibria. UV-visible absorption and fluorescence spectral data help to characterize the existence, in all cases, of excited-state intramolecular proton transfer (ESIPT) phenomena. Semi-empirical calculations involving full geometry optimization and calculation of heats of formation for the ground state (AM1) and vertical excitation energies and oscillator strengths (INDO/S) are in agreement with the experimental observations.

INTRODUCTION

Ground state proton transfer reactions are one of the simplest and most important processes found in chemistry.[1,2] The study of intramolecular proton transfer tautomerism has received increased attention in the last years, due to the characterization of a large number of cases where rapid hydrogen migration occurs not only in solution but also in the solid state.[3] In the latter case, the possibility exists that the materials could be used as a basis for devices capable of optical information storage.[4] Excited-state intramolecular proton transfer (ESIPT) reactions are of comparable importance both from theoretical and practical points of view.[5] Organic materials showing ESIPT phenomena are routinely used for photoprotection and photostabilization of polymers, for the UV protection of the human skin, etc.[6]

Anils of salicylaldehyde and other aromatic aldehydes are examples of compounds displaying both ground- and excited-state proton transfer processes which have been largely studied both in solution and in the solid state.[7–12] These compounds exist as an equilibrium mixture of the enol-imine form **a** and the keto-enamine form **b** in both phases (Scheme 1). The existence of ESIPT leads to a large Stokes' shift (ca. 10 000 cm^{-1}) between the absorption and fluorescence maxima, which can be explained through the so-called Förster cycles (Scheme 2).[13] Most of these compounds also present ESIPT in the crystalline phase, while a small group of them suffer a solid-state transformation on irradiation, yielding dark-colored products whose structure is still under some debate.[7,10] The latter process is known as photochromism, and is believed to be related to the crystalline space available for a *cis–trans* rearrangement of the excited state of tautomer **b**.

In the series of compounds **1–5**, i.e. *p*-substituted anils of salicylaldehyde, the dominant form is tautomer

* Authors for correspondence.

CCC 0894–3230/95/110713–08

Received 15 February 1995
Revised 13 June 1995

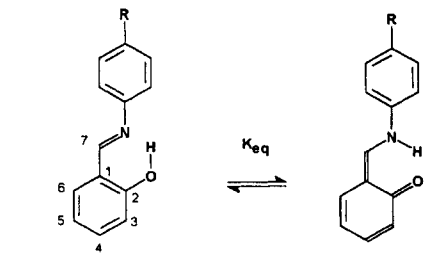

1 R = NMe_2
2 R = MeO
3 R = H
4 R = C(O)Me
5 R = NO_2

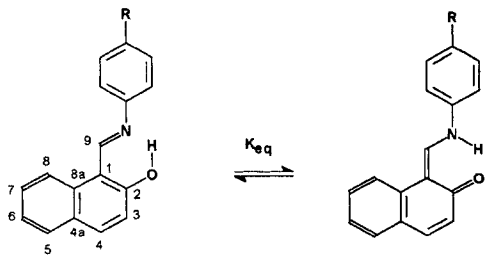

6 R = NMe_2
7 R = MeO
8 R = H
9 R = C(O)Me
10 R = NO_2

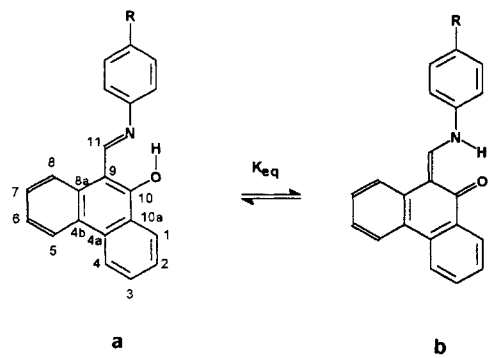

11 R = NMe_2
12 R = MeO
13 R = H
14 R = C(O)Me
15 R = NO_2

Scheme 1

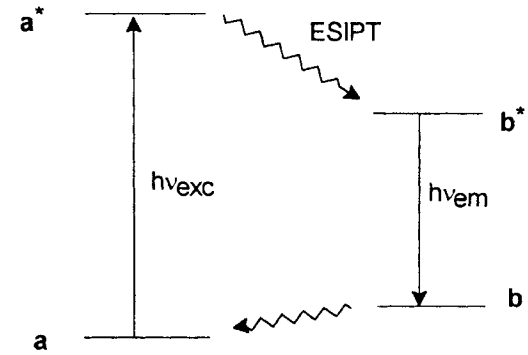

Scheme 2

a, as has been demonstrated by a variety of techniques,[9,11,12] whereas in the case of **6–10**, an equilibrium exists between forms **a** and **b** which is shifted towards the latter, and preserves significant amounts of form **a**.[11] We have recently reported the synthesis of **13**, which was shown to exist primarily as form **b**.[12] In the present work, we report a complete analysis of the spectroscopic results for the *p*-substituted series of novel Schiff bases **11–15**. Solution ^1H and ^{13}C NMR information has been used to establish the structure of the latter molecules, all of which can be considered as existing mainly as form **b**. In contrast to the case of **1–10**, the series **11–15** shows a consistent trend when changing the electronic demand of the substituent R, which agrees with the theoretical expectations.[11a] Also, variable-temperature ^{13}C NMR spectra were collected for compound **13** in order to further characterize the position of its tautomeric equilibrium.

We also report on both the experimental and theoretical aspects of ESIPT phenomena shown by compounds **1–15**. Electronic absorption and fluorescence spectroscopic measurements lead to the estimation of the Stokes' shifts, suggesting in all cases the presence of ESIPT cycles such as that shown in Scheme 2. Theoretical calculations of the properties of both ground (AM1) and excited (INDO/S) states of all the compounds studied are in good agreement with the experimental information.

EXPERIMENTAL

Melting points were obtained on a Electrotermal 9100 apparatus and are uncorrected. Infra-red spectra were recorded on a Bruker FT I-25 spectrophotometer. UV-visible absorption spectra were recorded on a Beckman DU 640 spectrophotometer and fluorescence spectra on a JASCO FP 770 spectrofluorimeter, in both cases using 1·00 cm quartz cuvettes. The concentration of the solutions studied (ethanol) ranged from 1×10^{-5} to 1×10^{-4} mol dm^{-3}.

Solution ^1H and ^{13}C NMR spectra were recorded on a

Bruker AC 200 NMR spectrometer operating at nominal frequencies of 200·1 and 50·3 MHz respectively. All chemical shifts were referenced against TMS. Low temperature measurements were performed by cooling the sample with evaporated liquid N_2. Temperatures were measured with a previously calibrated thermocouple, and are considered accurate within ±1 K.

Mass spectroscopic analyses were obtained at UMYMFOR, Universidad de Buenos Aires, on homogeneous samples verified by thin-layer chromatography on three solvent systems.

Ground-state geometry optimization and calculation of heats of formation and dipole moments was done by using the AMPAC package, version 2.10 on an 80486 microcomputer. In all cases the PRECISE option was used. Vertical excitation energies and oscillator strengths were calculated with the aid of INDO/S on the same microcomputer, including configuration interaction (CI) with the first 129 mono-excited singlet states.

The anils **1–15** were prepared by condensation of the appropriate aldehyde with the substituted aniline in refluxing methanol, followed by recrystallization. 9-Hydroxyphenanthrene-10-carbaldehyde was prepared as recently described.[12] Analytical data for the novel compounds **11–15** are as follows.

Compound **11**: m.p. 167–168 °C ($CHCl_3$); IR (KBr), ν 3050, 2922, 2849, 1619, 1605, 1526, 1499, 1388, 1311, 1192, 800, 753, 745 and 722 cm^{-1}; ^1H NMR ($CDCl_3$) δ 2·97 (s, NMe_2), 6·75 (d, J = 8·9 Hz, H3′ and H5′), 7·25 (d, J = 8·9 Hz, H2′ and H6′), 7·2–7·8 (overlap, mult., H2, H6 and H7), 7·70 (td, J = 7·1 and 1·5 Hz, H3), 7·92 (d, J = 8·0 Hz, H8), 8·36 (d, J = 7·2 Hz, H5), 8·40 (d, J = 8·0 Hz, H4), 8·53 (dd, J = 7·8 and 1·4 Hz, H1), 8·86 (d, J = 9·9 Hz, H11), 15·3 (br. d, J = 10 Hz, NH); ^{13}C NMR, see Table 1; MS, m/z (rel. int.), 340 (M^+, 65), 323 (9·5), 268 (10), 165 (12·5), 149 (14), 133 (7·5), 120 (16), 111 (10), 97 (22·5), 83 (48·5), 71 (54), 57 (100); found for M^+, 340·157461; $C_{23}H_{20}O_1N_2$ requires M^+, 340·157563.

Compound **12**: m.p. 168–169·5 °C (MeOH); IR (KBr), ν 3030, 2921, 1623, 1604, 1515, 1500, 1328, 1250, 1179, 1157, 1030, 818, 753 and 723 cm^{-1}; ^1H NMR ($CDCl_3$) δ 3·65 (s, OMe), 6·98 (d, J = 8·8 Hz, H3′ and H5′), 7·31 (d,J = 9·0 Hz, H2′ and H6′), 7·2–7·7 (overlap. mult., H2, H6 and H7), 7·71 (td, J = 7·0 and 1·4 Hz, H3), 7·89 (dd, J = 8·2 and 1·2 Hz, H8), 8·36 (dd, J = 7·4 and 1·4 Hz, H5), 8·39 (d, J = 7·4 Hz, H4), 8·57 (dd, J = 8·0 and 1·4 Hz, H1), 8·82 (d, J = 11·0 Hz, H11), 15·1 (br. d, J = 10·5 Hz,NH); ^{13}C NMR, see Table 1; MS, m/z (rel. int.), 327 (M^+, 97·5), 340 (34·1), 312 (14·6), 310 (10·2), 282 (3·9), 239 (3·4), 219 (4·8), 190 (9·7), 176 (13·6), 164 (39·0), 149 (17·0), 133 (9·7), 127 (10·7), 111 (12·2), 97 (20·9), 83 (65·8), 69 (68·3) and 57 (100).

Compound **13**: m.p. 133–134 °C (MeOH); IR (KBr), ν 3020, 2902, 1624, 1606, 1594, 1364, 1316, 854, 750 and 724 cm^{-1}; ^1H NMR ($CDCl_3$) δ 7·19–7·25 (mult., H4′), 7·32–7·50 (overlap. mult., H2′, H6′, H3′, H5′, H6 and H7), 7·56 (ddd, J = 8·0, 7·8 and 1·2 Hz, H2), 7·71 (ddd, J = 8·0, 7·1 and 1·4 Hz, H3), 7·89 (dd, J = 7·8 and 1·2 Hz, H8), 8·35 (dd, J = 8·0 and 1·3 Hz, H5), 8·38 (dd, J = 7·2 and 1·1 Hz, H4), 8·57 (dd, J = 7·8 and 1·4 Hz, H1), 8·88 (d, J = 11·2 Hz, H11), 14·8 (br. d, J = 11·2 Hz, NH); ^{13}C NMR, see Table 1; MS, m/z (rel. int.), 298 (M + 1, 8·9), 297 (M^+, 41·3), 296 (M − 1, 39·7), 165 (10·9), 97 (18·3), 95 (22·2), 81 (52·9), 69 (100), 55 (30·6) and 41 (23·7), found for M^+, 297·115494; $C_{21}H_{15}O_1N_1$ requires M^+, 297·115364.

Compound **14**: m.p. 201–202·5 °C (MeOH); IR (KBr), ν 3025, 2917, 1674, 1628, 1593, 1555, 1543, 1484, 1465, 1367, 1304, 1276, 1167, 1123, 961, 834, 818, 749 and 723 cm^{-1}; ^1H NMR ($CDCl_3$) δ 2·61 [s, C(O)Me], 7·37 (d, J = 8·6 Hz, H2′ and H6′), 7·35–7·59 (overlap. mult., H2, H6 and H7), 7·72 (td, J = 7·0 and 1·2 Hz, H3), 7·87 (dd, J = 7·6 and 1·2 Hz, H8), 8·03 (d, J = 8·6 Hz, H3′ and H5′), 8·31–8·34 (overlap. mult., H4 and H5), 8·52 (dd, J = 8·0 and 1·2 Hz, H1), 8·80 (d, J = 11·2 Hz, H11), 14·7 (br. d, J = 11 Hz, NH); ^{13}C NMR, see Table 1; MS, m/z (rel. int.), 339 (M^+, 10·0), 322 (1·3), 236 (4·9), 165 (4·4), 152 (5·4), 123 (68·3), 111 (12·2), 97 (29·3), 83 (51·2),

Table 1. Solution ^{13}C NMR chemical shifts for compounds **11–15**[a]

	COMPOUND				
CARBON	**11**	**12**	**13**	**14**	**15**
1	127·0	126·3	126·5	126·7	127·0
2	127·5	126·8	126·8	127·1	127·4
3	131·7	131·3	132·1	132·2	132·7
4	123·3	122·5	122·5	122·6	122·8
4a	135·7	133·3	135·8	133·4	136·3
4b	125·1	124·6	124·7	125·3	125·7
5	124·2	123·4	123·5	123·6	123·8
6	124·2	123·7	124·0	124·7	125·3
7	128·5	127·7	127·8	128·0	128·2
8	119·5	118·6	118·8	119·2	119·6
8a	131·3	132·2	132·1	131·7	132·6
9	105·2	104·9	105·4	106·7	107·9
10	179·3	179·8	181·0	182·4	182·5
10a	130·3	130·3	130·3	130·1	130·6
11	147·5	146·8	146·8	144·1	143·8
1′	133·3	135·2	139·0	135·7	146·4
2′,6′	120·3	119·5	117·9	117·0	117·3
3′,5′	113·8	115·0	129·7	130·4	125·9
4′	149·8	157·6	125·3	143·7	147·2
OMe		55·4			
NMe_2	41·1				
C(O)Me				26·3	
C(O)Me				196·3	

[a] Solvent: $CDCl_3$, except for **11** (CD_2Cl_2).

69 (59·5) and 55 (100), found for M^+, 339·125595; $C_{23}H_{17}O_2N_1$ requires M^+, 339·125929.

Compound **15**: m.p. 184–185 °C (MeOH); IR (KBr), ν 3057, 2410, 1626, 1584, 1565, 1555, 1500, 1330, 1315, 1305, 1266, 1244, 1109, 1029, 845, 742 and 721 cm^{-1}; ^1H NMR ($CDCl_3$) δ 7·43 (d, J = 9·0 Hz, H2 and H6'), 7·37–7·61 (overlap. mult., H2, H6 and H7), 7·76 (td, J = 8·4 and 1·5 Hz, H3), 7·89 (dd, J = 7·6 and 1·6 Hz, H8), 8·33 (d, J = 9·0 Hz, H2' and H6'), 8·31–8·37 (overlap. mult., H4 and H5), 8·52 (dd, J = 8·0 and 1·4 Hz, H1), 8·78 (d, J = 10·9 Hz, H11), 14·0 (br. d, J = 11 Hz, NH); ^{13}C NMR, see Table 1; MS, m/z (rel. int.), 342 (M^+, 100), 325 (5·8), 295 (31·7), 279 (7·8), 267 (4·8), 219 (5·3), 190 (5·8), 176 (7·8), 165 (18·0), 148 (10·2), 133 (11·7), 120 (8·2), 76 (6·3), 63 (8·2), and 50 (8·7); found for M^+, 342·100444; $C_{21}H_{14}O_3N_2$ requires M^+, 342·100442.

RESULTS AND DISCUSSION

Satisfactory ^1H NMR spectra were obtained for the newly reported compounds **11**–**15**. In all cases a signal was observed corresponding to the N–H proton appearing at ca. 15 ppm as a doublet (J = 10–11 Hz) coupled to the H11 proton, strongly suggesting that the dominant tautomeric form in these compounds is **b**. As previously discussed,[11a,12] the parameter of choice in order to study the position of the tautomeric equilibrium **a** = **b** is the chemical shift of the C–O carbon (C2 in **1**–**10** and C10 in **11**–**15**). Approximate extreme values for the enol-imine form are 160 ppm for **1**–**5**, 155 ppm for **6**–**10** and 150 ppm **11**–**15** (with due account of the increased shielding produced on this carbon when fused aromatic rings are added to salicylaldehyde). For the keto-enamine form **b**, on the other hand, model compounds are difficult to find. We have previously estimated a value of about 180 ppm for the C–O carbon in this form,[11a] which was confirmed by the study of **13** (181·0 ppm at 298 K; seeTable 1).[12] Table 1 collects the ^{13}C NMR assignments for **11**, **12**, **14** and **15**, based on comparisons with the values previously ascribed to the carbons of **13** on the basis of one- and two-dimensional ^{13}C spectra.[12] The results show that the latter anils exist mainly in the keto-enamine form **b**. However, an interesting trend is found in going from R = NMe_2 to R = NO_2: increasing the electron-withdrawing ability of R leads to a further shift of the equilibrium towards form **b**, as monitored by a progressive downfield in the chemical shift for the C–O carbon C10. This result has been previously anticipated on the basis of AM1 calculations (see below),[11a] and is in disagreement with early UV-visible absorption data for **1**–**5**.[7] It should be noticed that, as already reported,[11a] intrinsic SCS effects from the R group on the ^{13}C chemical shift of the C–O carbon are negligibly small. Further NMR evidence on the position of the latter equilibrium is provided by variable temperature ^{13}C data for **13** using CD_2Cl_2 as solvent. Only a minor downfield shift is detected in the equilibrium-sensitive carbon C10 on cooling the sample [T/K, δ(C10)/ppm: 315, 180·7; 295, 181·0; 275, 181·3; 265, 181·4] in agreement with the fact that compound **13** is expected to exist mainly as tautomer **b**. In comparison, a small upfield shift has been detected for the analogous carbon signal in **3**,[11a] while a considerably larger change (up to 4 ppm) was observed for **8**.[11a] All this information is in excellent agreement with the proposed structures for the presently studied compounds.

Table 2 summarizes the absorption data in ethanol for **1**–**15**. The observed values of ε at a specific wavelength λ are population averages given by:

$$\varepsilon_\lambda = (\varepsilon_{a,\lambda}[\mathbf{a}] + \varepsilon_{b,\lambda}[\mathbf{b}])/([\mathbf{a}] + [\mathbf{b}])$$
$$= (\varepsilon_{a,\lambda} + \varepsilon_{b,\lambda}K_{eq})/(1 + K_{eq}) \quad (1)$$

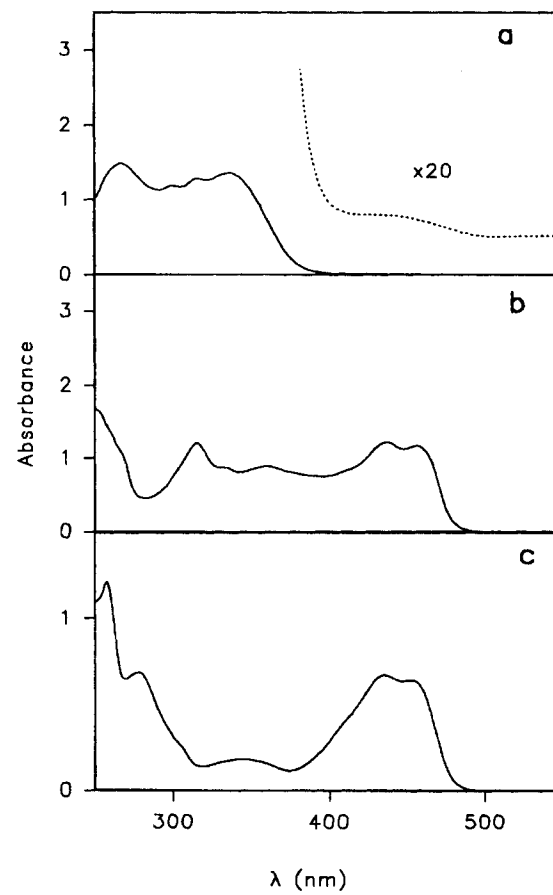

Figure 1. Absorption spectra of compounds which are representative of the three studied series of anils: (a) compound **3**, $1{\cdot}2 \times 10^{-4}$ M; (b) compound **8**, $4{\cdot}0 \times 10^{-5}$ M and (c) compound **13**, $1{\cdot}6 \times 10^{-5}$ M. All three solutions are in ethanol

where $\varepsilon_{a,\lambda}$ and $\varepsilon_{b,\lambda}$ are the extinction coefficients for tautomers **a** and **b** respectively at λ. Equation (1) can be simplified, however, if the observed maxima at 330–390 nm and 440–480 nm are ascribed to tautomers **a** and **b** respectively. Using compound **8** as an example, and assuming that the bands at 360 and 456 nm do not overlap:

$$\varepsilon_{360} = \varepsilon_{a,360}/(1 + K_{eq}) \quad (2)$$

$$\varepsilon_{456} = \varepsilon_{b,456}K_{eq}/(1 + K_{eq}) \quad (3)$$

This means that for ε to be a quantitative measure of the equilibrium displacement towards **b**, the intrinsic values $\varepsilon_{a,360}$ and $\varepsilon_{b,456}$ should be known in the solvent used. Since the latter values are not available, the foregoing discussion is necessarily qualitative as regards the relative populations of tautomers. Overall, however, the extinction coefficients of these bands are in agreement with the NMR information as regards the relative population of tautomers: **a** is predominant in **1–5**, **a** and **b** are comparable in **6–10**, and **b** dominates in **11–15**. Representative examples are shown in Figure 1. We have also determined the absorption coefficients of compounds **1–15** in $CHCl_3$ solution, in order to compare with the results obtained from ^{13}C NMR spectroscopy. The results are qualitatively similar to those found in ethanol, in the sense that the relative values of the extinction coefficients for the relevant absorption bands corresponding to tautomers **a** and **b** is maintained. In the series **1–5** and **11–15** the spectra are dominated by the absorption bands of tautomer **a** and **b** respectively. On the other hand, for the critical series of compounds **6–10**, in which substantial amounts of both forms exist, the observed values of ε in chloroform are: **6**, $\varepsilon_{320} = 11500$, $\varepsilon_{440} = 20200$; **7**, $\varepsilon_{386} = 14900$, $\varepsilon_{463} = 8800$; **8**, $\varepsilon_{372} = 9300$, $\varepsilon_{455} = 8400$; **9**, $\varepsilon_{386} = 6900$, $\varepsilon_{469} = 5800$; **10**, $\varepsilon_{349} = 16600$, $\varepsilon_{480} = 4300$.

Fluorescence results are also shown in Table 2. All compounds were excited at the wavelengths correspond-

Table 2. UV-visible absorptionand fluorescence data for compounds **1–15**[a]

	ABSORPTION		EMISSION[b]		STOKES' SHIFT
COMPOUND	λ_{max}/nm	ε	λ_{em}/nm	I_r	cm^{-1}
1	380	21800	545	440	8000
	470	600	545	830	2980
2	349	17000	540	1800	10180
	442	220	540	600	4180
3	336	11300	510	250	9800
	430	120	540	90	4700
4	343	10000	525	400	10100
	458	50	525	70	2800
5	354	12800	540	200	10100
	475	50	540	50	2800
6	376	2400	570	550	9100
	457	5330	570	250	4300
7	388	7000	525	9330	6700
	463	8330	525	23330	2600
8	360	6200	540	340	9300
	456	8600	540	400	3200
9	377	7000	500	3200	6500
	468	10000	500	6400	1400
10	370	25800	530	400	8200
	471	5200	530	550	2400
11	350	1580	550	2860	10400
	469	7400	560	11430	3500
12	342	5570	525	7580	10200
	444	21320	520	16360	3300
13	344	8940	514	4670	9600
	435	33300	514	9330	3500
14	357	6340	500	4330	8000
	446	25290	520	10000	3200
15	361	2240	525	1670	8700
	457	6460	530	3330	3000

[a] Solvent: ethanol, concentrations ranged from 1×10^{-5} to 1×10^{-4} mol dm^{-3}.
[b] In all cases, excitation was performed at the corresponding λ_{max}; I_r is computed as the ratio between the fluorescence intensity (in arbitrary units) to the concentration.

ing to the absorption of both **a** and **b**. In all cases fluorescence emission was obtained in the range 520–550 nm, irrespective of which band was irradiated. This implies the observation of a normal Stokes' shift when the band at longer wavelength is excited, but a much larger, ESIPT shift when the band corresponding to the absorption of **a** is excited (see Table 2). As with the electronic absorption measurements, the fluorescence intensity is only a qualitative measure of the values of K_{eq}. Absolute emission intensities by irradiating at a wavelength λ are given by:

$$I_\lambda = lP_0(\varepsilon_{a,\lambda}\phi_{a,\lambda}[\mathbf{a}] + \varepsilon_{b,\lambda}\phi_{b,\lambda}[\mathbf{b}]) = clP_0(\phi_{a,\lambda}\varepsilon_{a,\lambda} + \phi_{b,\lambda}\varepsilon_{b,\lambda}K_{eq})/(1 + K_{eq}) \quad (4)$$

where $c = [\mathbf{a}] + [\mathbf{b}]$ and $\phi_{a,b,\lambda}$ are the corresponding fluorescence quantum yields. Again referring to compound **8**, if the absorption bands at 360 and 456 nm are selectively irradiated, fluorescence will be emitted at 540 nm with the following intensities:

$$I_{r,360} = I_{360}/c = lP_0\phi_{a,360}\varepsilon_{a,360}/(1 + K_{eq}) \quad (5)$$

$$I_{r,456} = I_{456}/c = lP_0\phi_{b,456}\varepsilon_{b,456}K_{eq}/(1 + K_{eq}) \quad (6)$$

where $I_{r,\lambda}$ are the relative fluorescence intensities emitted at 540 nm when irradiation is performed at λ. These relative intensities are quoted in Table 2. Since the intrinsic values of $(\phi_{a,b,\lambda}\varepsilon_{a,b,\lambda})$ are not known, $I_{r,\lambda}$ cannot be taken as a quantitative measure of the value of K_{eq}. However, on a qualitative basis, the relative emission intensities of these bands (collected in Table 2) are in agreement with the expectations based on the relative populations of **a** and **b**. As seen in Table 2, the spectra for **1–5** are dominated by the ESIPT emission, those for **11–15** by the normal Stokes' shifted fluorescence, while **6–10** exhibit comparable intensities of the two bands. Compounds **1–5** exhibit a so-called 'reverse' energetic profile[5] (as the one depicted in Scheme 2), implying that $E_b > E_a$ while $E_{b^*} < E_{a^*}$. On the other hand, compounds **6–15** ar examples of 'normal' energy profiles (in the sense that $E_{b,b^*} < E_{a,a^*}$), especially in the case of the series **11–15**, in which **b** is the clearly dominating form in the ground state. The experimental ESIPT Stokes' shifts (see Table 2) for all three series of compounds are of comparable magnitude, implying that the factors which stabilize the keto-enamine form **b** on increasing the number of aromatic rings in the aldehyde moiety do also operate in producing a similar relative stabilization of the excited state $\mathbf{b}^*$ with respect to $\mathbf{a}^*$. This experimental result is in agreement (see below) with the theoretical calculations.

Semi-empirical calculations using the AM1 method are routinely used to study geometrical and thermodynamic properties of organic molecules, especially when hydrogen bonding occurs.[14] AM1 calculations have been previously shown to be in good agreement with the molecular geometries and relative energies of tautomers **a** and **b** in the case of **1–10** and also for **13**.[11a,12] We have optimized the geometries of **11**, **12**, **14** and **15**, with results which are comparable to those reported for **13**, i.e., tautomer **b** is preferred by ca. 25 kJ.mol^{-1}, in agreement with the NMR experiments (Table 3). The increased stability of the keto-enamine form **b** on increasing the number of fused aromatic rings in the aldehyde portion can be qualitatively pictured as follows. In compounds **1–5**, the aldehyde ring loses its aromaticity in going from **a** to **b**. In **6–10**,

Table 3. Ground-state (AM1) and excited-state (INDO/S) parameters for anils **1–15**

	TAUTOMER **a**		TAUTOMER **b**		$(E_{a^*} - E_{b^*})$
COMPOUND	λ/nm(f)[a]	ΔH_f^0/kJ.mol^{-1} (μ/D)	λ/nm(f)[a]	ΔH_f^0/kJ.mol^{-1} (μ/D)	cm^{-1}
1	316(1·00)	159·0 (3·47)	372(0·64)	177·8 (5·54)	3200
2	304(1·00)	−33·9 (1·41)	372(0·62)	−15·9 (3·47)	4500
3	306(0·32)	122·6 (2·21)	367(0·58)	140·6 (3·72)	3900
4	304(0·61)	−30·8 (2·03)	367(0·67)	−14·8 (0·52)	4300
5	314(1·00)	139·7 (6·02)	368(0·73)	156·9 (5·02)	3300
6	322(0·82)	23·4 (2·92)	369(0·14)	19·2 (4·64)	4300
7	317(0·68)	50·2 (2·99)	360(0·51)	46·0 (4·18)	4100
8	312(0·52)	208·4 (1·97)	354(0·53)	201·7 (3·09)	4400
9	319(0·84)	54·0 (2·62)	356(0·67)	46·7 (0·90)	3900
10	333(1·00)	225·9 (6·42)	355(0·79)	216·7 (5·81)	2600
11	324(0·83)	321·7 (2·44)	357(0·56)	298·2 (4·28)	4800
12	322(0·60)	126·0 (0·95)	356(0·29)	102·9 (2·36)	4900
13	320(0·41)	285·2 (1·45)	357(0·17)	260·0 (2·48)	5300
14	322(0·69)	130·6 (2·69)	353(0·26)	102·9 (1·17)	5000
15	329(0·93)	299·9 (6·70)	358(0·44)	273·8 (6·02)	4600

[a] In all cases the first allowed π–π^* singlet–singlet transition is quoted as the transition wavelength λ. The oscillator strength (f) is given in parentheses.

analysis of the contributing Kekule structures to the naphthalene portion shows that the unsubstituted ring is able to gain aromaticity in going from **a** and **b**. In this way the loss of aromaticity upon formation of the keto structure is balanced by its 'transfer' to the neighboring ring, a process which is not possible in **1–5**. Compounds **11–15** are even more liable for relieving the loss of aromaticity by transferring it to both fused aldehyde rings. As with **1–10**, the differences in heats of formation (a measure of the enthalpic change for the tautomeric reaction) predicts an increase in the population of the keto form **b** on increasing the electron-withdrawing ability of the substituent R [i.e. $\Delta(\Delta H_f^0)$ is about 3–4 kJ/mol smaller for $R = NO_2$ than for $R = NMe_2$ in the three series]. This is in contrast to early claims based on UV-visible absorption data for **1–5**.[9] In the case of compounds **11–15** the chemical shifts for the C–O carbon C10 reported in Table 1 appear to lend experimental support to the conclusions derived from the present semi-empirical calculations. A consistent downfield shift is detected in the equilibrium-sensitive carbon C10, implying a further shift towards **b** when the electron-withdrawing ability of the *p*-substituent is increased. It is interesting to note that although a similar trend has been previously predicted to occur for **1–10** on the basis of AM1 calculations, ^{13}C NMR information failed to reveal any significant change in the chemical shift of the equilibrium-sensitive carbon C2.[11a] These rather conflicting results could be explained by consideration of the AM1 calculated molecular dipole moments for **1–15** quoted in Table 3. Resorting to the Onsager classical electrostatic solvation model, the relative stabilizing solvation energy of **b** with respect to **a** is given by:[15]

$$\Delta E_s = [(D-1)/(2D+1)](\mu_b^2/r_b^3 - \mu_a^2/r_a^3) \qquad (7)$$

where $\mu_{a,b}$ are the dipole moments of forms **a** and **b**, $r_{a,b}$ are the cavity radii (which can be approximated by $r^3 = 3V/4\pi N_a$, V = molecular volume, N_a = Avogadro's number), and D is the solvent dielectric constant. In a given solvent, and assuming $r_a \approx r_b$, the magnitude of ΔE_s would be controlled by the difference $\Delta\mu^2 = \mu_b^2 - \mu_a^2$. Referring to the series of compounds **6–10**, $\Delta\mu^2$ is computed as (see Table 3): **6**, +13·0; **7**, +8·5; **8**, +5·7; **9**, −6·1; **10**, −7·5. Therefore, if $r_{a,b} \approx 5$ Å, $D = 4{\cdot}8$ ($CHCl_3$), the following values are calculated for ΔE_s (kJ/mol) for compounds **6–10**: 2·3, 1·5, 1·0, −1·1 and −1·3 respectively. With these values, the overall enthalpic changes for the tautomerization reaction are much less sensitive to the substituent effects. This implies that tautomers of type **a** would be relatively stabilized by the solvent with respect to **b** in going from $R = NMe_2$ to $R = NO_2$, an effect which would counterbalance the equilibrium drift predicted on the basis of the 'gas phase' ΔH_f^0 values reported in Table 3. The fact that the series **11–15** indeed shows the predicted equilibrium shift (as monitored by the chemical shift of C10, see above) may be due to their large molecular sizes. On one hand, the dipole moment contribution generated by the N–H···O moiety is buried within several aromatic rings. On the other, the large molecular volume of **11–15** (which may even include several $\pi-\pi$ stacked planar molecules) may diminish the effects brought about by differences in dipole moments for both tautomers, making these molecules approach a 'gas phase' behavior. If, for example, $r_{a,b}$ increases by 30% in going from the series **6–10** to **11–15**, the values of ΔE_s computed from equation (7) for the latter series would be negligibly small. To test this hypothesis, spectroscopic (both electronic absorption and NMR) information is being gathered for **1–15** in a variety of solvents, and the results will be compared with those for the related arylazonaphtholic system, in which significant substituent-induced equilibrium shifts have been reported.[3f] In the latter case, AM1-calculated dipole moments are always larger for the N–H tautomer (type **b**) than for the O–H tautomer (type **a**). These results will be published elsewhere.[16]

With the ground-state geometries of both tautomers of **1–15** fully optimized by AM1, excited-state calculations were done by means of INDO/S calculations. This method is used to calculate vertical excitation energies and oscillator strengths for organic molecules, and represents an improved version of the CNDO/S method.[17] The combination of ground-state calculations with AM1 and excited-state studies with INDO/S has already been shown to account for ESIPT phenomena in 3-hydroxyflavone and related compounds.[18] The relevant results obtained for the presently studied series of compounds are collected in Table 3. We focus on $\pi-\pi^*$ electronic transitions since the absorption bands for tautomers of types **a** and **b** have large extinction coefficients (see Table 2 which gives good approximations for ε_a in **1–5** and for ε_b in **11–15**, since these two series of compounds are dominated by the enol-imine and keto-enamine tautomers respectively). The first $\pi-\pi^*$ allowed electronic transition in tautomer **a** lies, in all cases, at shorter wavelengths than those corresponding to **b**, in agreement with the experiments. The calculated vertical excitation energies lie in the range 30 000–32 800 cm^{-1} for tautomers **a** and 26 900–28 300 cm^{-1} for **b**. In comparison with the experimental transitions (see Table 2, 25 700–29 800 cm^{-1} for **a** and 21 000–23 200 cm^{-1} for **b**), INDO/S overestimates them by ca. 4000 cm^{-1}, a result which is similar to that previously reported for 3-hydroxyflavone.[18] Combining the results for both ground and excited states, the relative energy of the excited states $\mathbf{a}^*$ and $\mathbf{b}^*$ can be obtained, and in all cases it is found (see Table 3) that $E_{b^*} < E_{a^*}$ irrespective of the relative energies of the ground states structures **a** and **b** ($E_a < E_b$ in **1–5**, $E_a \approx E_b$ in **6–10** and $E_a > E_b$ in **11–15**). This means that the semi-empirical calculations are able to predict ESIPT phenomena as a likely explanation for the shifts

observed between excitation and emission in the studied compounds. The calculated values of $(E_{a^*} - E_{b^*})$ are in agreement with the fact that the relative stabilization of the keto-enamine form **b** increases in going to the phenanthrene derivatives **11–15** (Table 3), as anticipated above. Furthermore, the calculated transition energies can be used to estimate the relative energy difference $[(E_a - E_{a^*}) - (E_{b^*} - E_b)]$, which is 5400, 3700 and 3200 cm^{-1} for the unsubstituted compounds **3**, **8** and **13** respectively. These magnitudes can be compared with the experimental values [in cm^{-1}, calculated from the differences in $(10^7/\lambda_{max})$ between both absorption bands, see Table 3]: 6500(**3**), 5800(**8**) and 6100(**13**). The comparison is satisfactory, keeping in mind that the calculated values are only accurate to within ±2000 cm^{-1}.

CONCLUSION

We have characterized five novel anils obtained by reaction of 9-hydroxyphenanthrene-10-carbaldehyde with *p*-substituted anilines. The structures of these compounds have been established in solution by means of ^1H and ^{13}C NMR spectroscopy, in the latter case at variable temperature. All these anils exist mainly in the keto-enamine tautomeric form. UV-visible absorption and fluorescence measurements are in agreement with the proposed structures, and are compared with corresponding data for anils of salicylaldehyde and 2-hydroxynaphthalene-1-carbaldehyde. In all cases both ESIPT and normal Stokes'-shifted emission bands are detected, with relative intensities which are in agreement with the ground-state populations estimated from the NMR data. Semi-empirical calculations of both ground (AM1) and excited (INDO/S) states lend further support to the experimental observations.

ACKNOWLEDGMENTS

We acknowledge financial support from the University of Rosario, CONICET (Consejo Nacional de Investigaciones Cientiíficas y Técnicas, Argentina) and Fundación Antorchas. S.H.A. and G.L. thank CONICET for Fellowships.

REFERENCES

1. P. Schuster, G. Zundel and C. Sandorfy (Eds), *The Hydrogen Bond. Recent Developments in Theory and Experiments*, North Holland, Amsterdam (1976).
2. J. Emsley, *Struct. Bonding (Berlin)* **57**, 147 (1984); *J. Chem. Soc. Revs.* **9**, 91 (1980); F. Hibbert and J. Emsley, *Adv. Phys. Org. Chem.* **26**, 255 (1991).
3. (a) L. Frydman, A. C. Olivieri, L. E. Diaz, A. Valasinas and B. Frydman, *J. Am. Chem. Soc.* **110**, 5651 (1988); (b) B. Wehrle, H. H. Limbach and H. Zimmermann, *Ber. Bunsen-Ges. Phys. Chem.* **91**, 941 (1987); (c) J. A. Smith, B. Wehrle, F. Aguilar-Parrilla, H.-H. Limbach, M. C. Foces-Foces, F. Hernandez Cano, J. Elguero, A. Baldy, M. Pierrot, M. M. T. Khurshid and J. B. Larcombe-McDouall, *J. Am. Chem. Soc.* **111**, 7304 (1989); (d) R. M. Cravero, M. González-Sierra and A. C. Olivieri, *J. Chem. Soc. Perkin Trans.* **2**, 1067 (1993); (e) S. H. Alarcón, A. C. Olivieri and P. Jonsen, *J. Chem. Soc. Perkin Trans.* **2**, 1783 (1993); (f) A. C. Olivieri, R. B. Wilson, I. C.Paul and D. Y. Curtin, *J. Am. Chem. Soc.* **111**, 5525 (1989).
4. B. L. Feringa, W. F. Jager and B. De Lange, *Tetrahedron* **49**, 8267 (1993).
5. (a) L. G. Arnaut and S. J. Formosinho, *J. Photochem. Photobiol. A: Chem.* **75**, 1 (1993); (b) S. J. Formosinho and L. G. Arnaut, *J. Photochem. Photobiol. A: Chem.* **75**, 21 (1993).
6. J. Catalán, F. Fabero, M. S. Guijarro, R. M. Claramunt, M. D. Santa María, M. C. Foces-Foces, F. Hernández Cano, J. Elguero and R. Sastre, *J. Am. Chem. Soc.* **112**, 747 (1990).
7. (a) T. Inabe, N. Hoshino, T. Mitani and Y. Maruyama, *Bull. Chem. Soc. Jpn.* **62**, 2245 (1989); (b) T. Inabe, *New. J. Chem.* **15**, 129 (1991); (c) N. Hoshino, T. Inabe, T. Mitani and Y. Maruyama, *Bull. Chem. Soc. Jpn.* **61**, 4207 (1988); (d) T. Inabe, I. Gautier-Luneau, N. Hoshino, K. Okaniwa, H. Okamoto, T. Mitani, U. Nagashima and Y. Maruyama, *Bull. Chem. Soc. Jpn.* **64**, 801 (1991); (e) T. Inabe, I. Luneau, T. Mitani, Y. Maruyama and S. Takeda, *Bull. Chem. Soc. Jpn.* **67**, 612 (1994); (f) T. Inabe, N. Hoshino-Miyajima, I. Luneau, T. Mitani and Y. Maruyama, *Bull. Chem. Soc. Jpn.* **67**, 622 (1994).
8. J. Seliger, V. Zagar, R. Blinc, E. Hadjoudis and F. Milia, *Chem. Phys.* **142**, 237 (1990).
9. J. W. Ledbetter Jr, *J. Phys. Chem.* **72**, 4111 (1968).
10. (a) M. D. Cohen and G. M. J. Schmidt, *J. Phys. Chem.* **66**, 2442 (1962); (b) E. Hadjoudis, M. Vittorakis and I. Moustakali-Mavridis, *Tetrahedron* **43**, 1345 (1987).
11. (a) S. H. Alarcón, A. C. Olivieri and M. González-Sierra, *J. Chem. Soc. Perkin Trans.* **2**, 1067 (1994); (b) S. R. Salman, J. C. Lindon, R. D. Farrant and T. A. Carpenter, *Magn. Reson. Chem.* **31**, 991 (1994).
12. S. H. Alarcón, A. C. Olivieri, G. R. Labadie, R. M. Cravero and M. González-Sierra, *Tetrahedron* **51**, 4619 (1995).
13. Th. Förster, *Z. Elektrochem.* **54**, 42 (1950); *Naturwiss.* **36**, 186 (1949).
14. M. J. S. Dewar, E. G. Zoebisch, E. F. Healy and J. J. P. Stewart, *J. Am. Chem. Soc.* **107**, 3902 (1985).
15. M. M. Karelson, A. R. Katritzky, M. Szafran and M. C. Zerner, *J. Org. Chem.* **54**, 6030 (1989).
16. S. H. Alarcón and A. C. Olivieri (in preparation).
17. R. L. Ellis and J. J. Jaffé, *J. Mol. Spectrosc.* **50**, 474 (1974).
18. B. Dick, *J. Phys. Chem.* **94**, 5752 (1990).